Novel Electrochemical Biosensor based on Cationic Peptide Modified Hemin/G-quadruples Enhanced Peroxidase-like Activity

Qian Yu, Yongmei Wu, Zi Liu, Sheng Lei, Gaiping Li, Baoxian Ye

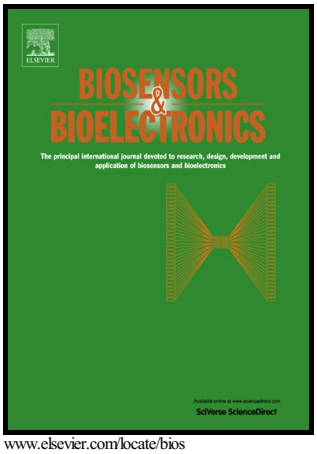

www.elsevier.com/locate/bios

PII: S0956-5663(18)30100-3
DOI: https://doi.org/10.1016/j.bios.2018.02.014
Reference: BIOS10276

To appear in: *Biosensors and Bioelectronic*

Received date: 13 November 2017
Revised date: 2 February 2018
Accepted date: 2 February 2018

Cite this article as: Qian Yu, Yongmei Wu, Zi Liu, Sheng Lei, Gaiping Li and Baoxian Ye, Novel Electrochemical Biosensor based on Cationic Peptide Modified Hemin/G-quadruples Enhanced Peroxidase-like Activity, *Biosensors and Bioelectronic,* https://doi.org/10.1016/j.bios.2018.02.014

Novel Electrochemical Biosensor based on Cationic Peptide Modified Hemin/G-quadruples Enhanced Peroxidase-like Activity

Qian Yu, Yongmei Wu*, Zi Liu, Sheng Lei, Gaiping Li, Baoxian Ye*

College of Chemistry and Molecular Engineering, Zhengzhou University, Zhengzhou 450001, PR China

Abstract:

This work designed an artificial substrate peptide to synthesize peptide-hemin/G-quadruplex (peptide-DNAzyme) conjugates. In addition to enhancing catalytic activity of hemin/G-quadruplex, the peptide could also be induced and cleaved by prostate specific antigen (PSA). It was the first report on peptide-DNAzyme conjugates in application of the peptide biosensor. The polyethyleneimine-reduced graphene oxide@hollow platinum nanotubes (PEI-rGO@PtNTs) nanocomposites were cast on the glassy carbon electrode in order to form the interface of biocompatibility and huge surface area for bioprobes immobilization. In absence of PSA, the peptide-DNAzyme conjugates retained intact on the surface of the electrode to produce a strong response signal. But in presence of PSA, the peptide-DNAzyme conjugates were destroyed to release electron mediators, resulting in dramatical decrease of the electrochemicl signal. Therefore, the method had high sensitivity and super selectivity with the limit of detection calculated as 2.0 fg/mL. Furthermore, the strategy would be promising to apply for other proteases

* Corresponding author. Tel.: +86 0371 67781757; fax: +86 0371 67763654.

E-mail address: yebx@zzu.edu.cn (B. X. Ye); wuyongmei0001@163.com (Y. M. Wu).

by transforming the synthetic peptide module of target.

Keywords: Peptide-DNAzyme conjugates, Prostate specific antigen, Peptide biosensor, Signal amplification

1. Introduction

G-quadruplex (GQ) is formed from the mutual interaction of the deoxyguanosine-rich motifs within single-strand DNA via Hoogsteen H-bonding with the aid of sodium-potassium (Wang et al., 1991; Wang et al., 2009). Hemin as an interactive agent interacts with intramolecular GQ structure by direct stacking to or intercalating with G-tetrads in formation of hemin/G-quadruplex (hGQ) (Zhang et al., 2001; Han et al., 1999). It is well known that the hGQ owns the superiority of easy labeling, less cost, and great structure stability against hydrolysis and heat treatment (Limoges et al., 2008; Chen et al., 2018). To date, the hGQ has been proved to possess horseradish peroxidase-mimicking (HRP-mimicking) activity (Travascio et al., 1999). Hence, the hGQ serves as novel catalyst to be widely used for the development of various biosensors (Li et al., 2017; Lu et al., 2017; Yuan et al., 2017). For instance, Chen et al. developed an electrochemical method to detect thrombin based on hGQ (also named DNAzyme) with octahedral Cu_2O-Au nanocomposites for signal amplification (Chen et al., 2018). Gao et al. designed the proximity-dependent recombination of hGQ for label-free and signal-on electrochemical assay DNA (Gao et al., 2017). Shi et al. integrated catalytic hairpin assembly (CHA) with terminal deoxynucleotidyl transferase (TdT)-mediated in situ DNA polymerization in

formation of hGQ to highly sensitive and label-free measure thrombin in human serum (Shi et al., 2017).

Despite there are the overwhelming majority of researches on hGQ utilized extensively in DNAzyme sensors for signal amplification (Tang et al., 2016; Wang et al., 2017; Tang et al., 2012; Zhou et al., 2017; Ravan et al., 2017), few essays about hGQ with special peptide of target are applied to build peptide biosensors for detection of various targets. Up till now, the hGQ's relatively lower catalytic activity than that of native horseradish peroxidase seriously restricts its further development and application. In an effort to enhance the peroxidase-mimicking activity of the GQ for improving the performance of the sensor (Feng et al., 2017; Guo et al., 2017), Xiao et al. developed that cationic peptide covalently bound with the NH_2 terminal of GQ to stabilize the secondary structure of GQ, to enhance the binding affinity of the hemin and to further improve mimic peroxidase activity of DNAzyme (Xiao et al., 2016). In this regard, our group previously proposed an effective electrochemical aptamer by cationic peptide conjugate GQ (TBA aptamer) with enchanced the peroxidase-like activity of DNAzyme to ultrasensitive assay the thrombin (Wu et al., 2017), but some drawbacks of this method, such as a more-sophisticated label of the second aptamer, longer-time fabrication and easily loss catalyzed activity of peptide-hGQ conjugates, might result in the lower stability and reproducibility of the biosensor and even limit its further wide application. To circumvent these limitations, we herein designed an artificial substrate peptide to synthesize peptide-hGQ conjugates in application of the peptide biosensor for the first time.

In this work, the artificial substrate peptide was modified hGQ through Michael addition to construct the peptide biosensor. The artificial substrate peptide composed two domains: a positively charged, histidine-rich domain conjugated with GQ in formation of peptide-GQ conjugates for signal amplification and the special peptide of prostate specific antigen (PSA) (HSSKLQ). PSA enabled to induce and cleave HSSKLQ for label-free and ultrasensitive electrochemical detection of PSA. Additionally, the polyethyleneimine-reduced graphene oxide@hollow platinum nanotubes (PEI-rGO@PtNTs) nano-composites were deposited on the surface of the electrode not only to offer sensors with large electroactive surface area and enhanced electronic properties, but also to boost the efficiency of probe-target complexation and the rate of electrochemical reactions (Wu et al., 2013). Furthermore, hemin was used as signal tag avoiding the addition of extra electron mediators for the matrix contamination. Scheme 1 indicated the schematic diagram of biosensor for PSA assay. First, with the help of the excellent film-forming property of Nafion, the PEI-rGO@PtNTs were modified on the surface of the glassy carbon electrode (GCE) to availably improve electrical conductivity and enhance the active-area of the electrode. Then the peptide-hGQ conjugations were immobilized on the PEI-rGO@PtNTs/GCE by covalent interaction. Next, the blocking reactant hexanethiol (HT) was dropped on the surface of the modified electrode to reduce a higher incidence of non-specific binding to target. In absence of the target, the biosensor was measured to conclude a sensitive electrochemical signal, which was from the redox of hemin. After incubating with target, PSA specially cut peptide-hGQ

conjugates into two fragments (peptide1 and peptide-hGQ conjugates2). The peptide1 remained on but peptide-hGQ conjugates2 were released from the surface of the modified electrode. So the electrochemical signal reduced sharply. Therefore, the developed biosensor had a large detection range for PSA from 5 fg/mL to 20 ng/mL with the detection limit of 2.0 fg/mL. The designed peptide biosensor also enabled to assay PSA in human serum. The synthetic peptide module could be easily replaced by the substrate peptide of other protein proteases. Therefore, this method had the potential to be a versatile platform for protein protease assay.

2. Experiment section

2.1. Materials and experiment measurements

Prostate specific antigen (PSA), hexanethiol (HT), chloroplatinic acid hexahydrate ($H_2PtCl_6 \cdot 6H_2O$), gold(III) chloride hydrate ($HAuCl_4$), and sulfosuccinimidyl-4-(N-maleimidomethyl) cyclohexane-1-carboxylate (sulfo-SMCC) were acquired from Sigma-Aldrich Chemical Co. (St. Louis, MO, USA). Graphene oxide (GO) was purchased from Nanjing XianFeng Nano Co. (Nanjing, China). Polyethyleneimine (PEI), tellurium dioxide (TeO_2, 99.9%), hydrazine monohydrate, hexadecyltrimethylammonium bromide (CTAB, 99%), sodium dodecyl sulfate (SDS, 99%) and Glutaraldehyde (GA) were obtained from Aladdin Co. Ltd. (Shanghai, China). G-quadruplex (GQ) with the sequence of 5′-GTGGGTAGGGCGGGTTGGAAAAAA-NH_2-3′ was synthesized by Sangon, Biotech Co.; Ltd. (Shanghai, China). The peptide (CAAAHHHHHHSSKLQ) was synthesized by Shanghai Science Peptide Biological Technology Co.; Ltd (Shanghai,

China). 0.1 M phosphate buffered solution (PBS, pH 7.0 if not otherwise stated) as the supporting electrolyte was prepared by mixing the stock solution of 0.1 M Na_2HPO_4 0.1 M KH_2PO_4, and 0.1 M KCl. Buffer A (conjugation buffer): 500 mM NaCl, 100 mM Na_2HPO_4-NaH_2PO_4, pH 7.3. Buffer B (enzyme reaction buffer): 200 mM NaCl, 50 mM HEPES, 0.03% Triton X-100, 20 mM KCl, pH 7.0. Other reagents were of analytical grade and used as received. Ultrapure water with electrical resistance 18.2 MΩ•cm was obtained from Thermo Scientific Barnstead GenPure water purification system (Thermo Fisher Scientific Co.; Ltd, Shanghai, China), and used throughout experiments. Besides specified, otherwise, the solutions for experiments were ultrapure water. Additionally, the human serum was used for real sample analysis and was obtained from the First Affiliated Hospital of Zhengzhou University (Henan, China).

Electrochemical measurements were performed at room temperature using one CHI 650 A electrochemical workstation (Shanghai Chenhua Instrument, China) in a standard three-electrode cell containing 4 mm-diameter glassy carbon working electrode, a platinum counter electrode and a Ag/AgCl (3 M KCl) reference electrode (CHI). Experimental datas were collected using differential pulse voltammetry (DPV) in 2 mL PBS (0.1 M, pH 7.0) containing 9.8 mM H_2O_2 from -0.5 V - 0.1 V in increments of 0.1 V vs. Ag/AgCl with an amplitude of 50 mV, pulse width of 0.05 s and sample width of 0.0167 s and Cyclic voltammetry (CVs) were conducted in the PBS (pH 7.0) as supporting electrolyte. The surface morphology characterization of nanomaterials was performed by using transmission electron microscope (TEM)

micrographs (USA FEI, M3000) and scanning electron microscopy (SEM, JEOL, JSM-7500F). The absorption spectra were recorded on Lambda 35 Ultraviolet–visible (UV–Vis) spectrophotometer using a quartz glass cuvette with 1 cm path length (Pgeneral General Instrument, Beijing, China). The pH measurements were taken with a PHS-3C precision pH meter (Shanghai, China). CD spectra were often used to measure the 10 μM GQ or peptide-GQ conjugates (40 μL 100 μM of GQ or peptide-GQ conjugates were put into in buffer B to acquire 400 μL 10 μM GQ or peptide-GQ conjugates) at 25 ^{o}C on a Chirascan Plus spectropolarimeter over the range of 220-320 nm using a 1 cm path length quartz cuvette. In CD or absorbance melting temperature (T_m) experiments, the samples were heated from 20 to 95 ^{o}C at a rate of 2 ^{o}C/min, and CD signals were recorded at each ^{o}C. PAGE gel (20% denatured by 8M urea) analysis was achieved by about 5 μL 15 μM GQ/peptide-GQ conjugates under 250 V. Finally, the obtained gel was stained by Stains-All from Sigma-Aldrich Co. Ltd.

2.2. Synthesis of PEI-rGO@PtNTs

Synthesis of PEI-rGO

To synthesize the PEI-rGO (Cao et al., 2010), firstly, 1mL 3% PEI was added into 10 mL 1.0 mg/mL graphene oxide dispersion under magnetic stirring. Then the intermixture was reacted at 135 ℃ for 3 h. The black produce should be centrifuged and washed for several times. The obtained product was noted as PEI-rGO, which was of good solubility.

Synthesis of hollow PtNTs

According to the previous method to prepare PtNTs, Te nanowires (TeNWs) serving as reducing agents and sacrificial templates were first synthesized (Cai et al., 2013). 5 mL hydrazine hydrate was added into a small beaker containing 32 mg TeO_2. The additive process was drop by drop and then the mixture was stirred constantly for 1 h. The obtained solution was added into 45 mL 10 mM SDS solution with a proper stirring speed for 3 mins. The productions were centrifuged and rinsed several times with ultrapure water to gain the TeNWs. Next, the TeNWs were dispersed in 25 mL 1 mM CTAB solution. The mixture was stirred for 15 mins, followed by quickly addition of an amount of H_2PtCl_6 solution (pH 7.0, NaOH solution was utilized to adjust the pH for H_2PtCl_6 solution) with constant stirring for 50 mins. The productions could be collected by the centrifugation and washing several times, and then were redispersed into 500 μL ultrapure water to stand for 3 h. Finally, the gained solution was centrifuged and washed to obtained PtNTs.

An amount of PtNTs was added into 2 $mg.mL^{-1}$ PEI-rGO mixed liquor (isopropanol : water : Nafion (5%) = 1:1:0.005) with constant stirring overnight to get the PEI-rGO@PtNTs (Choi et al., 2010; Sun et al., 2017).

2.3. Synthesis of peptide-hGQ conjugates

The peptide conjugate GQ was prepared according to the previous report (Xiao et al., 2016). 2 mg sulfo-SMCC was dispersed into buffer A containing 200 μL 100 μM GQ (PS2.M), with the mixture on roller for 2 h at room temperature. The production was filtered and rinsed six times with buffer A through an Amicon-3K ultrafilter (3 kDa cutoff) to remove excessive sulfo-SMCC. The GQ activated by sulfo-SMCC was

synthesized. 2 mg peptide was added into 200 μL 100 μM the activated GQ. The mixture reacted for 48 h. The peptide covalently bound with activated GQ to form the peptide-GQ conjugates. The obtained substance was centrifuged and washed six times by buffer A.

0.5 mg hemin was added into 100 μL 100 μM the peptide-GQ conjugates and reacted for 30 mins to prapare the peptide-hGQ hydrids, which were stored under -20 °C to use.

2.4. Fabrication of PSA biosensor

It was essential that the GCE was activated. First, the electrode was polished by 0.03 μm-diameter alumina slurries, and followed by sonication in ultrapure water and alcohol. After that, 2 μL the PEI-rGO@PtNTs were dropped on the surface of the GCE and were dried by N_2. Then 10 μL 10 μM peptide-hGQ conjugates were covered on the surface of PEI-rGO@PtNTs/GCE and incubated overnight at room temperature. Finally, 20 μL HT was dropped on the modified electrode to block the remaining active site for 50 mins in humidity, and then rinsed by ultrapure water to get the designed biosensor. When not used, the prepared biosensor was stored under 4 °C.

3. Result and discussion

3.1. Characterization of PEI-rGO@PtNTs

In this study, the PEI-rGO@PtNTs were prepared to be used as superb platform for biomaterials loading. From IR image (Fig. 1A), the absorption peak of C=O for the PEI-rGO dramatically decreased at 1730 cm^{-1} versus that of the GO, which suggested the chemical bind of PEI to the GO (Cai et al., 2012). To further verify the reduction

of GO to PEI-rGO, the ultraviolet experiments were done. In Fig. 1B, GO showed a strong adsorption peak at 230 nm due to the π to π* transition of aromatic C–C bond. But the characteristic UV-visible absorption peaks of GO at 230 nm and 300 nm shifted to 268 nm (Zhang et al., 2011), because the conversion of the GO to the PEI-rGO did not destroy the aromatic structure within the GO nanosheets. Thus, we could draw a conclusion that when PEI was regarded as reductant, the reduction of GO was achieved. In addition, the TEM of PEI-rGO illustrated PEI-rGO with excellent dispersity in ultrawater (the inset of Fig. 1B). Fig. 1D was the TEM image of PtNTs, indicating that the diameter and the longth of PtNTs were about 20 nm, around 260 nm respectively and they were hollow nanotubes structure. And TeNWs served as a sacrificial templates for the synthesis of PtNTs (the TEM image was in Fig. 1C). All results demonstrated that PEI-rGO@PtNTs were elegantly made.

To characterize the electrochemical activity of the PEI-rGO@PtNTs, the electrochemical experiments were carried out through cyclic voltammetry (CV) method in 5 M $[Fe(CN)_6]^{3-/4-}$ solution. As shown in Fig. 2A, both the reductive/oxidation peak currents of the PEI-rGO@PtNTs/GCE efficiently increased versus the bare GCE, which ascribed to the distinct superiority of PEI-rGO@PtNTs, such as large specific surface area, fine electroconductibility, nice biocompatibility and so on.

3.2. Characterization of peptide-hGQ conjugates

According to the precious reports about GQ, Circular dichroism (CD) spectra were often used to analyze the secondary structure of the GQ. Thus, circular dichroism (CD)

experiments were done in HEPES solution containing K^+ for demonstrating the conformation of GQ and peptide-GQ conjugates. As shown in Fig. S2 (A), three characteristic peaks of GQ were 295 (+) nm, 260 (+) nm, 245 (-) nm respectively. The peak intensities of peptide-GQ conjugates increased greatly at 245 (-) nm and 260 (+) nm, but another decreased sharply and even disappeared completely (Yang et al., 2011) compared with those of the GQ. According to the previously reports, the two peaks at 260 (+) nm, 245 (-) nm were the typical characteristic of parallel GQ (Burge et al., 2006), the appearance of positive peak at 296 nm shown in form of antiparallel GQ structure (Xu et al., 2015). And the parallel GQ had higher DNAzyme activity than that of the antiparallel GQ (Xiao et al., 2016). The above results indicated that the conformation of GQ was successfully formed (Cheng et al., 2009) and peptide-GQ conjugates were synthesized prettily. We could prove that the peptide covalent modified GQ almost entirely produced parallel GQ structures with enhanced electrocatalysis activity. The peptide-GQ conjugates were also verified using PEAG (Polyacrylamide gel electrophoresis) (Lu et al., 1993). As shown in Fig. S2 (B), bright bands were observed on the lanes where activated GQ and peptide-GQ conjugates were line 2 and line 3 respectively. The peptide-GQ conjugates obviously had lower electrophoretic mobility than GQ alone (Lane 3 vs. Lane 2) owing to the lower molecular weight of GQ versus peptide-GQ conjugates, proving the formation of peptide-GQ conjugates.

3.3. Characterization of the biosensor interfaces

The electrochemical methods were utilized to characterize the step-by-step of

biosensor using the PBS (pH 7.0) as electrolyte solution. As shown in Fig. 2B, the curve a (the bare GCE) had no redox peak. And then the PEI-rGO@PtNTs were cast on the electrode surface, there was still no redox peak observed but we could observe that the ESA was increased (the curve b). When peptide-hGQ conjugates (bioprobes) were immobilized on the surface of the modified electrode, the obvious peak current could be produced (curve c) suggesting signal tag (hemin) attached to the surface of the modified electrode successfully. To further add the the blocking reagent (HT), the current dramatically decreased (curve d) and the corresponding potential difference increased, indicating sluggish electron-transfer kinetics through non-conductng micromolecules on the surface of the modified electrode. After the targets were incubated for a period, the electrical signal continued to decrease (curve e), showing that the peptide-hGQ conjugates were induced and cleaved by PSA resulting in the decrease of their peak current. All experiment datas indicated that the PSA peptide biosensor was established greatly.

3.4. Strategy of this biosensor for signal amplification

To verify the aforementioned signal enhancement was attributed to intrinsic peroxidase-like activity of peptide-hGQ conjugates, we designed the different modified electrodes, which were immersed in PBS (pH 7.0) with or without H_2O_2 through DPV method to evaluate the feasibility of the biosensor for signal application under same experimental conditions. In the following control experiments, we expected to observe the excellent electrocatalysis of peptide-hGQ conjugates. As shown in Fig. 2C, the curve a had no peak current at the PEI-rGO@PtNTs/GCE, but

the curve b (Fig. 2C) at the HT/peptide-hGQ conjugates/PEI-rGO@PtNTs/GCE had an excellent reductive peak current in PBS (pH 7.0) without H_2O_2. As expected, the I value was more lower than the value of reductive peak current obtained at the HT/peptide-hGQ conjugates/PEI-rGO@PtNTs/GCE in PBS (pH 7.0) with H_2O_2 (the curve b in Fig. 2C vs. the curve c in Fig. 2D). And the difference between the curve b and the curve c was around 9 μA. It clearly demonstrated that the proposed peptide-hGQ conjugates were able to efficiently enhance the sensitivity. This also gave the key evidence that the peptide-hGQ conjugates led to a dramatic signal amplification. The enhanced effect might be due to that cationic peptide modification not only to stabilize anionic GQ structure, but also to improve the hemin binding affinity to GQ (Chang et al., 2016; Qi et al., 2014a; Xiao et al., 2016). Herein, the biosensor for signal application was feasible.

3.5. Quantification of PSA

The developed biosensor was incubated with different concentration of PSA. The acquired experiment datas were in Fig. 3. The DPV currents decreased gradually as the concentration of the PSA ranged from 5 fg/mL to 20 ng/mL. The regression equation could be expressed as follows:

$I = 1.990 \lg c_{PSA} - 12.14$, $R = 99.20$ %

R^2 was linear correlation coefficient. The limit of detection (LOD) was estimated to be 2.0 fg/mL (S/N=3). Hence, we proved that the fabricated biosensor could be used to quantification of PSA. We then compared with the previously reported biosensors (Tang et al., 2017; Strzemińska et al., 2016; Hun et al., 2015; Xie et al., 2015; Qi et al.,

2014b; Zhou et al., 2018; Zhao et al., 2018; Li et al., 2015) (Table 1), showing peptide-hGQ conjugates-based peptide biosensor with better sensitivity, which might ascribe to cationic peptide modified hGQ with enhanced mimicking-peroxidase activity for efficiently improving the analytical performance of the peptide biosensor. And compared with other peptide-based PSA biosensors, the approach had a larger detection range, ascribing to the enhanced peroxidase-like activity of peptide-hGQ conjugates and no addition of extra electron mediators.

3.6. The selectivity, reproducibility of the biosensor

The five biosensors were assayed the concentration of the interferences (thrombin (TB), carcinoembryonic antigen (CEA), Bovine serum albumin (BSA)), PSA and the mix. As showed in Fig. S4, the electrochemical signals for the interferences (100 ng/mL) were almost equal, but the electric currents of PSA (10 ng/mL) and the mix sharply decreased, demonstrating excellent selectivity of the developed method. Then we also investigated the reproducibility of proposed biosensor by using four electrodes under the same condition. The relative standard deviation (RSD) was 8.86% under the same condition, proving a good reproducibility of the proposed electrochemical biosensor.

3.7. Quantification of PSA in human serum sample

In order to verify the reliability and applicability of this proposed strategy for clinical analysis, the electrochemical experiments were carried out through standard addition method in human serum sample (obtained from the First Affiliated Hospital of Zhengzhou University, China). The human serum sample was firstly diluted 100

time and then 0.07 ng, 0.5 ng, 2 ng, 5 ng, 20 ng were spiked into 1 mL diluted human sample respectively to prepare several samples. The results were all in Table S1. The analytical recoveries obtained in real serum samples were from 94.85% to 108.2% and the RSD values were from 1.26% to 8.15%, indicating that the developed biosensor could be applied to assay PSA in real sample successfully.

4. Conclusions

In summary, a new peptide electrochemical biosensor for label-free and sensitive detection of PSA was developed based on cationic peptide modified hGQ. The artificial peptide covalent binding with GQ not only efficiently enhanced peroxidase-mimicking activity of GQ, but also constructed bioprobe induced and cleaved by PSA to avoid the fussy label process of peptide. And PEI-rGO@PtNTs nanocomposites offered load platform with large electroactive surface area and enhanced electronic properties. This method was simple and did not need complex operation to achieve label-free and sensitive detection of PSA. And with the aid of H_2O_2, the method enabled to obtain analytical signals inside the dynamic range of 5 fg/mL-20 ng/mL, but could not be applied to direct measure PSA in human serum. The proposed strategy would be promising to apply for other proteases assay by transforming the synthetic peptide module of target.

Acknowledgements

The authors are sincerely grateful for the financial support from the National Natural Science Foundation of China (No: 21575130).

References

Bai, L.J., Yuan, R., Chai, Y.Q., Yuan, Y.L., Wang, Y., Xie, S.B., 2012. Chem. Commun. 48, 10972-10974.

Burge, S., Parkinson, G.N., Hazel, P., Todd, A.K., Neidle, S., 2006. Nucleic Acids Res. 34, 5402–5415.

Cai, X., Lin, M.S., Tan, S.Z., Mai, W.J., Zhang, Y.M., Liang, Z.W., Lin, Z.D., Zhang, X.J., 2012. Carbon 50, 3407-3415.

Cai, K., Lv, Z.C., Chen, K., Huang, L., Wang, J., Shao, F., Wang, Y.J., Han, H.Y., 2013. Chem. Commun. 49, 6024-6026.

Cao, L.Y., Liu, Y.L., Zhang, B.H., Lu, L.H., 2010. ACS Appl. Mater. Interfaces 2, 2339-2346.

Chang, T.J., Gong, H.M., Ding, P., Liu, X.J., Li, W.G., Bing, T., Cao, Z.H., Shangguan, D.H., 2016. Chem Eur J 22, 4015-4021.

Chen, S., Liu, P., Su, K.W., Li, X., Qin, Z., Xu, W., Chen, J., Li, C.R., Qiu, J.F., 2018. Biosens. Bioelectron. 99, 338-345.

Cheng, X.H., Liu, X.J., Bing, T., Cao, Z.H., Shangguan, D.H., 2009. Biochemistry 48, 7817-7823.

Choi, B.G., Park, H.S., Park, T.J., Yang, M.H., Kim, J.S., Jang, S.Y., Heo, N.S., Lee, S.Y., Kong, J., Hong, M.W.H., 2010. ACS Nano 4, 2910-2918.

Feng, M.L., Ruan, Z.Y., Shang, J.C., Xiao, L., Tong, A.J., Xiang, Y., 2017. Bioconjugate Chem. 28, 549-555.

Guo, Y.H., Chen, J.L., Cheng, M.P., Monchaud, D.D., Zhou, D.J., Ju, H.X., 2017. Angew. Chem. Int. Ed. 56, 16636-16640.

Gao, F.L., Fan, T.T., Wu, J., Liu, S., Du, Y., Yao, Y., Zhou, F.Y., Zhang, Y., Liao, X.J., Geng, D.Q., 2017. Biosens. Bioelectron. 96, 62-67.

Han, F.X., Wheelhouse, R.T., 1999. J. Am. Chem. Soc. 121, 3561-3570.

Hun, X., Xu, Y.Q., Luo, X.L., 2015. Microchim Acta 182, 1669-1675.

Li, J.L., He, G.W., Mu, C.L., Wang, K.M., Xiang, Y., 2017. Anal. Chem. 986, 131-137.

Li, J.X., Ma, H.M., Wu, D., Li, X.J., Zhao, Y.B., Zhang, Y., Du, B., Wei, Q., 2015. Biosens. Bioelectron. 74, 104-112.

Li, T., Wang E.K., Dong S.J., 2009. Chem. Eur. J. 15, 2059-2063.

Limoges, B., Marchal, D., lectrodes, F., 2008. J. Am. Chem. Soc. 130, 7259-7275.

Lu M., Guo Q., Kallenbach N.R., 1993. Biochemistry 32, 598-601.

Lu, S.S., Wang, S., Zhao, J.H., Sun, J., Yang, X.R., 2017. Anal. Chem. 89, 8429-8436.

Qi, C., Zhang, N., Yan, J.L., Liu, X.J., Bing, T., Mei, H.C., Shangguan, D.H., 2014a. RSC Adv. 4, 1441.

Qi, H.L., Li, M., Dong, M.M., Ruan, S.P., Gao, Q., Zhang, C.X., 2014b. Anal. Chem. 86, 1372-1379.

Ravan, H., Amandadi, M., Esmaeili-Mahani, S., 2017. Anal. Chem. 89, 6022-6029.

Shi, K., Dou, B.T., Yang, J.M.,Yuan, R., Xiang, Y., 2017. Biosens. Bioelectron. 87, 495-500.

Sun, Y.J., Luo, M.C., Meng, X.X., Xiang, J., Wang, L., Ren, Q.S., Guo, S.J., 2017. Anal. Chem. 89, 3761-3767.

Strzemińska, I., Fanchine, S.S.R., Anquetin, G., Reisberg, S., Noël, V., Pham, M.C., Piro, B., 2016. Biosens. Bioelectron. 81, 131-137.

Tang, G.E., Zhao, C.L., Gao, J., Tan, H.L., 2016. Sens. Actuators B 237, 795-801.

Tang, J., Hou, L., Tang, D.P., Zhang, B., Zhou, J., Chen, G.N., 2012. Chem. Commun. 48, 8180-8182.

Tang, Z.X., Fu, Y.Y., Ma, Z.F., 2017. Biosens. Bioelectron. 94, 394-399.

Travascio, P., Bennet, A.J., Wang, D.Y., Sen, D., 1999. Chem. Biol. 6, 779-787.

Wang, C.Y., Qian, Y., Zhang, Y., Meng, S.Y., Wang, S.Y., Li, Y.H., Gao, F.L., 2017. Sens. Actuators B 238, 434-440.

Wang, R., Wang, A.J., Liu, W.D., Yuan, P.X., Xue, Y.D., Luo, X.L., Feng, J.J., 2018. Biosens. Bioelectron.102,

276-281.

Wang, Y., Santos, C.D.L., Gao, X.L., Greene, K., Live, D., Patel, D.J., 1991. J. Mol. Biol. 222, 819-432.

Wu, Y.M., Zou, L.N., Lei, S., Yu, Q., Ye, B.X., 2017. Biosens. Bioelectron. 97, 317-324.

Wu, Y.M., Xu, W.J., Bai, L.J., Yuan, Y.L., Yi, H.Y., Chai, Y.Q., Yuan, R., 2013. Biosens. Bioelectron. 50, 50-56.

Xiao, L., Zhou, Z.J., Feng, M.L., Tong, A.J., Xiang, Y., 2016. Bioconjugate Chem. 27, 621-627.

Xie, S.B., Zhang, J., Yuan, Y.L., Chai, Y.Q., Yuan, R., 2015. Chem. Commun., 51, 3387--3390.

Xu, H.Y., Geng, F.H., Wang, Y.X., Xu, M.T., Lai, X.H., Qu, P., Zhang, Y.T., Liu, B.H., 2015. Chem. Commun. 51, 8622−8625.

Yang, X.J., Fang, C.L., Mei, H.C., Chang, T.J., Cao, Z.H., Shangguan, D.H., 2011. Chem. Eur. J. 17, 14475-14484.

Yuan, R., Yu, X.L., Zhang, Y.H., Xu, L.L., Cheng, W., Tu, Z.G., Ding, S.J., 2017. Biosen. Bioelectron. 92, 342-348.

Zhang, Y.L., Shen, H.X., Zhang, C.X., Ottova, A. L., Tien, H.T., 2001. Electrochim Acta 46, 1251-1257.

Zhang, Y., Chen, B., Zhang, L.M., Huang, J., Chen, F.H., Yang, Z.P., Yao, J.L., Zhang, Z.J., 2011. Nanoscale 3, 1446.

Zhao, J.C., Ma, Z.F., 2018. Biosens. Bioelectron. 102, 316-320.

Zhou, Q., Lin, Y.X., Zhang, K.Y., Li, M.J., Tang, D.P., 2018. Biosens. Bioelectron. 101. 146-152.

Zhou, X.X., Guo, S.J., Gao, J.X., Zhao, J.M., Xue, S.Y., Xu, W.J., 2017. Biosens. Bioelectron. 98, 83-90.

Research highlights

- An artificial peptide modified hGQ was first applied in electrochemical peptide biosensor to detect prostate specific antigen (PSA).
- An artificial peptide contained one cationic peptide enhancing peroxidase activity of hGQ and the special peptide induced and cleaved by PSA.
- The novel peptide biosensor exhibited a wide linear range, low detection limit, excellent selectivity and high sensitivity.

Figure Captions

The schematic diagram of biosensor for PSA assay.

Fig. 1 The IR (A) and UV-visible (B) characterization of PEI-rGO and GO. The inset in Fig. 1B was the TEM image of PEI-rGO. The TEMs of TeNWs (C); hollow PtNTs (D).

Fig. 2 (A) The CV curves of 5 mM $[Fe(CN)_6]^{3-/4-}$ solution at the PEI-rGO@PtNTs/GCE (a) and GCE (b).

(B) The electrochemical characterization of the different modified electrodes in 0.1 M PBS (pH 7.0). GCE-a; PEI-rGO@PtNTs/GCE-b; peptide-hGQ conjugates/PEI-rGO@PtNTs/GCE-c; HT/peptide-hGQ conjugates/PEI-rGO@PtNTs/GCE-d; the biosensor after incubating PSA-e.

(C) The DPV of the PEI-rGO@PtNTs/GCE (a) and HT/peptide-hGQ conjugates/PEI-rGO@PtNTs/GCE after incubating PSA in 0.1 M PBS (pH 7.0) without 9.8 mM H_2O_2 (b).

(D) The DPV of the PEI-rGO@PtNTs/GCE (a) and HT/peptide-hGQ conjugates/PEI-rGO@PtNTs/GCE after incubating PSA in 0.1 M PBS (pH 7.0) with 9.8 mM H_2O_2 (c).

Fig. 3 (A) Differential pulse voltammetry (DPVs) of the developed biosensor for quantifying PSA in 0.1 M PBS (pH 7.0) containing 50 μL 9.8 mM H_2O_2. (B) Calibration curve of DPV peak response on the logarithm of different PSA concentration.

Table 1 Comparison of different biosensors for PSA assay.

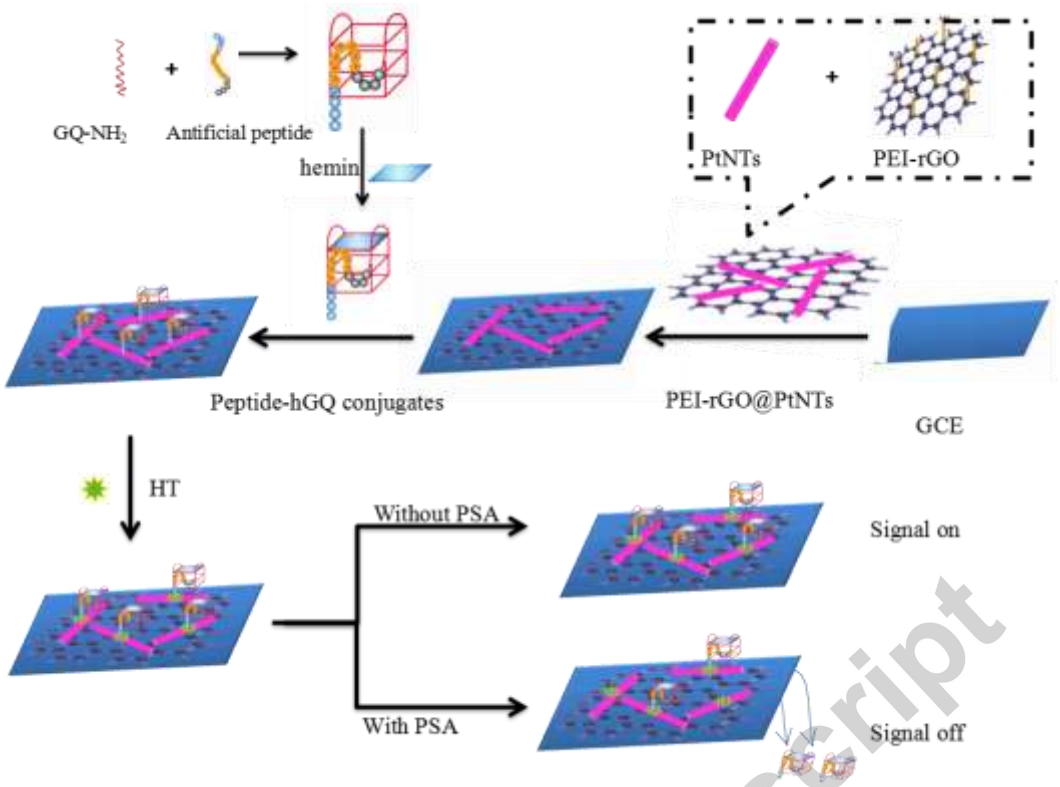

Scheme 1

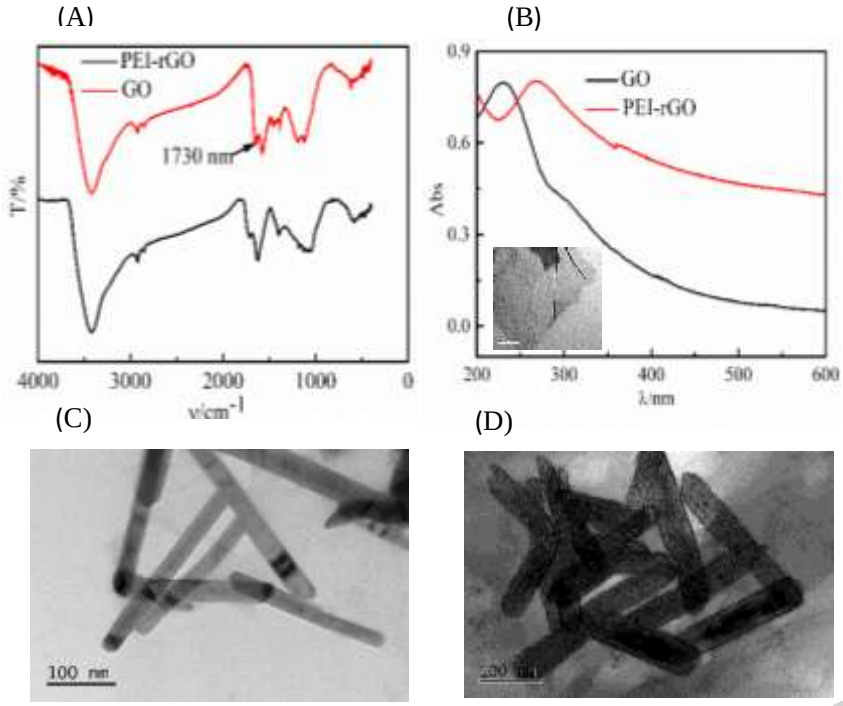

Fig. 1

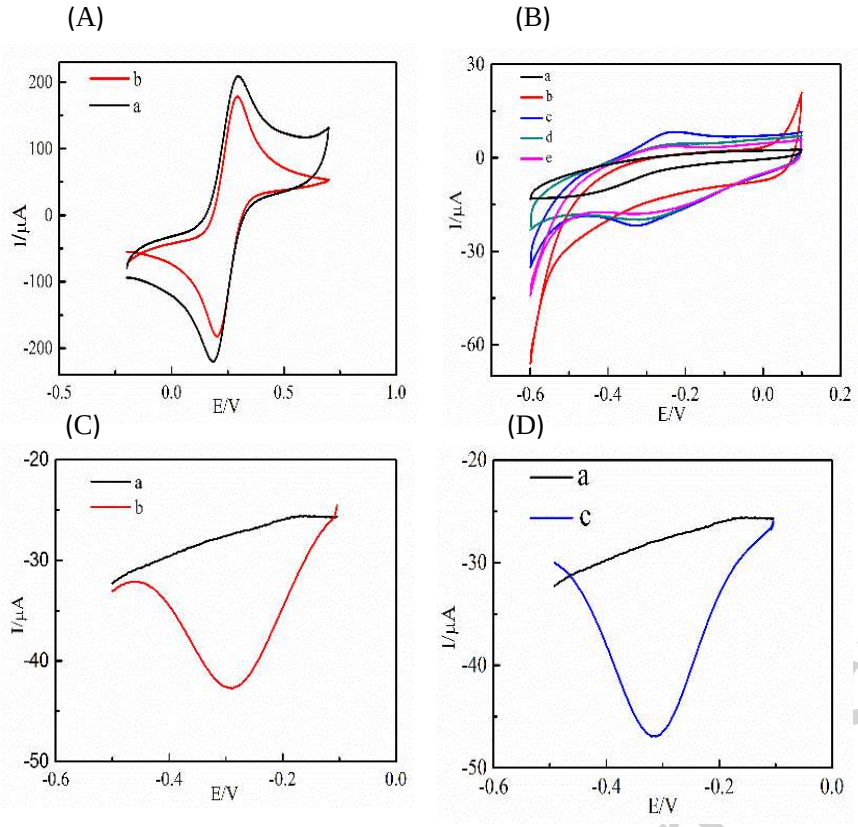

Fig. 2

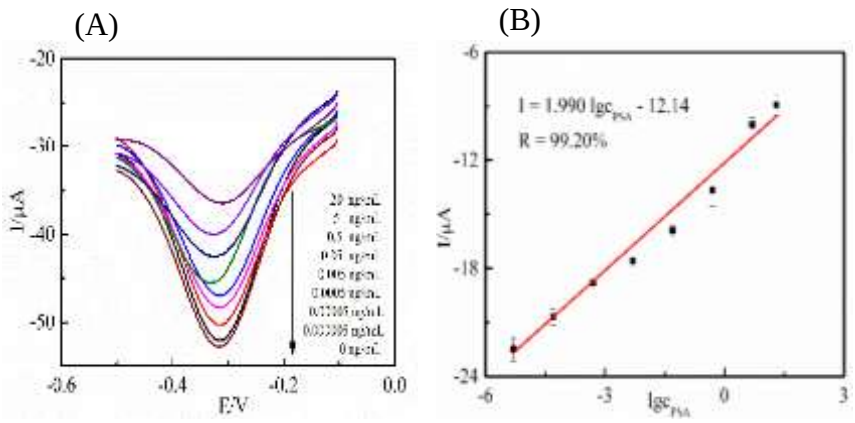

Fig. 3

Table 1 Comparison of different biosensors for PSA detection

Biosensor	Method	Detection Range (ng/mL)	Detection Limit (pg/mL)	References
Aptasensor	Photoelectrochemistry	1×10^{-3}-100	0.31	Zhou et al. 2018
Aptasensor	Electrochemistry	1×10^{-5}-100	0.0023	Zhao et al. 2018
Immunosensor	Electrochemiluminescence	5×10^{-3} -5	3	Li et al. 2015
Peptide biosensor	Electrochemistry	33-33 $\times10^{6}$	-	Strzemińska et al. 2016
Peptide biosensor	Electrochemistry	8×10^{-2}-7	30	Hun et al. 2015
Peptide biosensor	Electrochemistry	1×10^{-3}-30	0.78	Xie et al. 2015
Peptide biosensor	Electrochemiluminescence	5×10^{-3}-5	0.8	Qi et al. 2014b
Peptide biosensor	Electrochemistry	5×10^{-6}-20	0.002	This work